Thompson[2] has advocated a slightly different approach in which electrons are effectively localized in the metal anion. However, the recent optical studies of thin films of lithium with methylamine by Dye and co-workers[57] show no absorptions which can be attributed to Li^-.

Summary

In the previous sections we have discussed the relationship between the vapor–liquid condensation that accompanies the cooling of an alkali-metal gas, and the liquid–liquid phase separation in metal–ammonia and lithium–methylamine solutions. Table I is a collation of critical (consolute) densities in lithium– and sodium–ammonia solutions and lithium–methylamine solutions together with the observed critical densities of the pure alkali metals and the corresponding estimates of the Mott criterion for all systems under investigation.

These condensation phenomena observed in both the gaseous and matrix-bound systems appear to be closely related. Furthermore, they are significantly correlated in that, in all cases, critical (metal) densities at the metallic onset are in good agreement with the Mott criterion (eq 3, Table I). The slightly different constants found for the two solvent systems may possibly be related[21] to differences in the nature of the (host) conduction band; but any further considerations must await more detailed experimental and theoretical studies of the localized, excess electron in lithium–methylamine solutions. However, there is evidence[30] to suggest that the slightly lower constant of ca. 0.26 found for metal–ammonia solutions and the wide variety of highly doped semiconductors,[20] as compared with the value of ca. 0.30–0.34 found for the expanded fluid alkali metals (Table I), may be related to the proximity of an unoccupied (host) conduction band in the matrix-bound systems.

In summary, we suggest that the observed condensation phenomena for both gaseous and matrix-bound alkali metals are indeed a direct manifestation of the major electronic constitution change at the M–NM transition.[16,17] Thus, the critical Mott density in these systems signals the onset of an electronic transition *without* a thermodynamic phase transition for temperatures above a certain critical temperature, T_c. This critical density is also that at which a thermodynamic phase change accompanies the electronic transition below T_c.

It is also apparent that Pitzer's suggestion[7] that phase separation in metal–ammonia solutions is the analogue within the liquid-ammonia medium of the liquid–vapor separation of the pure metal does indeed represent a particularly apt description of the phenomenon. In this context, we have attempted to stress the fundamental importance[20] of the localized-electron entity in dictating the composition for the electronic/thermodynamic transition.

We are still, however, no nearer any reasonable explanation for the *absence* of phase separation in cesium–ammonia solutions.[2] Expanded fluid cesium does indeed show a two-phase regime[9-11] with a critical point[23] at a density of 0.42 g cm^{-3} and a temperature of 2023 K. In addition, electrical, transport, and magnetic properties indicate that the M–NM transition is closely correlated with both the Mott density and the liquid–gas critical point.[11,30] Cesium is miscible in all proportions in liquid ammonia near room temperature, and measurements of electrical and magnetic properties reveal a M–NM transition in the range 4–5 MPM. However, there is *no* evidence[61] for liquid–liquid phase separation in this system. This is even more intriguing in view of recent magnetic susceptibility studies[30,58] of metallic and nonmetallic expanded fluid cesium which reveal notable similarities with the corresponding magnetic behavior in metal–ammonia solutions in the approach to the metallic state.[59,60]

Acknowledgment. This research was sponsored by the National Science Foundation under Grant No. DMR-78-12238 and was supported in part by the Air Force Office of Scientific Research and the Materials Science Center at Cornell University. P.P.E. wishes also to acknowledge the support of the Science Research Council.

(57) Dye, J. L.; DaGue, M. G.; Yemen, M. R.; Landers, J. S.; Lewis, H. L. *J. Phys. Chem.* **1980**, *84*, 1096.

(58) Freyland, W. *Phys. Rev. B: Condens. Matter* **1979**, *20*, 5104.
(59) Mott, N. F. *J. Phys. Chem.* **1980**, *84*, 1203.
(60) Edwards, P. P. *Phys. Chem. Liq.*, in press.
(61) See also: Even, U.; Swenumson, R. D.; Thompson, J. C. *Can. J. Chem.* **1977**, *55*, 2240 and references therein.

Chemical Reaction Paths. 7.[1] Pathways for S_N2 and S_N3 Substitution at Sn(IV)

Doyle Britton*[2a] and Jack D. Dunitz*[2b]

Contribution from the Organic Chemistry Laboratory, Swiss Federal Institute of Technology, ETH-Zentrum, CH-8092 Zürich, Switzerland. *Received June 2, 1980*

Abstract: Reaction pathways involving four-, five- and six-coordinated Sn(IV) are derived from an examination of 186 crystal structures found from a search of the Cambridge Crystallographic Data Centre Database. For the reaction $Y + SnR_3X \rightleftharpoons [YSnR_3X] \rightleftharpoons YSnR_3 + X$, the structure correlation method provides a convincing mapping of the S_N2 pathway with inversion of configuration. The S_N2 pathway with retention of configuration is not so well-defined, but some of its features are revealed. For the reaction $2Y + SnR_2X_2 \rightleftharpoons [Y_2SnR_2X_2] \rightleftharpoons Y_2SnR_2 + X_2$, there is a well-defined pathway involving a symmetrical double addition and elimination process. We call this type of termolecular reaction an S_N3 reaction and show that it can be distinguished from alternative reaction types with the same stoichiometry. Structures involving seven- and eight-coordinated Sn(IV) are briefly mentioned. The somewhat meager data for Ge(IV) and Pb(IV) are discussed in the Appendix.

While tetraorganotin compounds RR′R″SnR‴ are optically stable, triorganotin halides are not.[3] This has been explained by the tendency of the triorganotin compounds in the presence of nucleophiles to expand their coordination number to form stereochemically nonrigid five- or six-coordinated intermediates or

(1) Part 6. Bürgi, H. B.; Shefter, E.; Dunitz, J. D. *Tetrahedron* **1975**, *31*, 3089–3092.
(2) (a) On sabbatical leave from University of Minnesota, Chemistry Department, Minneapolis, MN 55455. Address correspondence to him there. (b) To whom correspondence should be addressed at the Swiss Federal Institute of Technology.
(3) Gielen, M.; Hoogzand, C.; Simon, S.; Tondeur, Y.; Van den Eynde, I.; Van de Steen, M. In "Organotin Compounds: New Chemistry and Applications"; Zuckerman, J. J., Ed.; ACS: Washington, DC, 1976; pp 249–257.

0002-7863/81/1503-2971$01.25/0

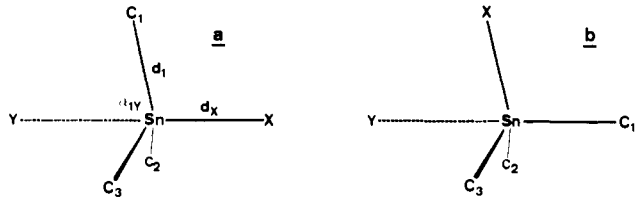

Figure 1. Possible directions of approach of nucleophilic group Y to SnR_3X (only the C atom bonded to Sn is shown in each R group): *a*, opposite X; *b*, opposite R, adjacent to X (this approach is required if X and Y are part of the same bidentate ligand).

by direct inversion of configuration via an S_N2 mechanism.[3,4] Information about possible, low-energy interconversion paths is desirable.

In this paper we apply the structure correlation method[5] to organometallic tin compounds, our main aim being to map such pathways between four- and five-coordinate Sn and between four- and six-coordinate Sn. In this method, the structural parameters of relevant molecular fragments are examined to see if they vary in a systematic manner. If correlations are found, the correlation functions so obtained can be assumed to trace paths that roughly follow potential energy valleys in the appropriate parameter space. The interpretation of such paths as chemical reaction paths rests essentially on analogy, on the general similarity between the patterns of molecular deformations found in crystal environments and the changes in molecular structure that are associated with chemical reactions.

For the change from four- and five-coordination, there is an obvious chemical analogy: the formation of the transition state or intermediate in the S_N2 type of displacement. In principle such displacements can occur with retention or inversion of configuration at the central atom depending on whether the incoming group is cis or trans to the leaving group (see Figure 1). At carbon, S_N2 displacement invariably occurs with inversion, but both kinds of path may be possible for other elements. Bürgi[6] has mapped out the inversion path of tetrahedral Cd(II) from a study of CdS_3XY ensembles.

For the change from four- to six-coordination, we have no kinetic or mechanistic analogy since the three-body collision that would be involved in the corresponding chemical reaction is highly unlikely.[7] In crystal environments, however, nominally tetrahedral molecules of type R_2MX_2 are often coordinated to two additional ligands Y. From systematic studies of such ensembles we can hope to map pathways for what we may refer to as S_N3 types of displacement.

$$MR_2X_2 + 2Y \rightleftharpoons [MR_2X_2Y_2] \rightleftharpoons MR_2Y_2 + 2X$$

In principle there are now three main variants, assuming that the Y atoms tend to approach the centers of triangular faces of the C_2MX_2 tetrahedron in the R_2MX_2 molecules (Figure 2): (a) both Y atoms approach the C_2X faces, each remaining opposite to an X atom, to give an octahedral transition state or intermediate with C_{2v} microsymmetry and with trans R groups or (b) both Y atoms approach the CX_2 faces, each remaining opposite to an R group, to give again an intermediate with C_{2v} microsymmetry but with trans X atoms or (c) one Y atom approaches an C_2X face and the other approaches an CX_2 face, the first remaining opposite to an X atom and the second remaining opposite to an R group, giving an intermediate with C_1 microsymmetry and with cis R groups, cis X atoms, and cis Y atoms. There is no way the approach of two Y atoms to the faces of an C_2MX_2 tetrahedron can lead to an octahedral structure with trans R, trans X, and trans Y groups.[8] Most of the $R_2SnX_2Y_2$ examples that are actually found correspond to possibility a with trans R groups.

We have used the Cambridge Crystallographic Database[9] to examine the crystal structures of organotin compounds. Of the 24 127 entries in the bibliographic file as of August 1979, 297 cover tin-containing compounds. After structures based on two-dimensional data, those with serious disorder, and those for which no coordinates are given were eliminated, there are 186 entries that refer to Sn(IV) compounds. These provide 250 examples of Sn(IV) atoms in various chemical environments. We first classify these 250 examples, next consider bond lengths in general, and finally examine correlations and reaction pathways. Ge(IV) and Pb(IV) are considered in the Appendix. For a recent review of the structural chemistry of tin, see Zubieta and Zuckerman,[10] who describe and picture many of the compounds used in this survey. Some aspects, particularly the relation to Mössbauer spectroscopic results, have been discussed by Harrison.[11]

A Preliminary Look at the Data

We now consider briefly each class of tin environment SnC_nZ_m, where Z is any element or elements other than carbon; Z_m does not imply *m* identical atoms but only *m* atoms other than C. In the discussions of each class we shall use X to represent electronegative elements and M to represent metallic ones.

A classification based on coordination number requires for each ensemble a decision as to what atoms are bonded to the Sn atom. While this is usually clear-cut, it is not always so. Our procedure was to identify as possible ligands all atoms whose distance from the Sn atom was within 1.3 A of the relevant standard single bond distance, $d_X(1)$ (see section on standard bond lengths). The four atoms whose distances were closest to $d(1)$ were always defined as ligands. The remaining possible ligands were examined one-by-one to see whether their nearness to Sn was a trivial consequence of their attachment to previously chosen ligands. If so, the ligand in question was eliminated; otherwise it was included. Groups such as acetate with one O atom much closer to Sn than the other present obvious problems. Except in the most extreme cases, the higher coordination number was assigned.

Two other problems of classification were: (a) what is Sn(IV) and (b) when should a C atom be called an X atom? We classify as Sn(IV) any Sn atom having only shared electron pairs (i.e., no lone pairs) in its valence shell. For example, we classify the ion $SnCl_3^-$ as containing Sn(II) and the ensemble $MoSnCl_3$ as containing Sn(IV). Murray-Rust, Bürgi, and Dunitz[12] have shown for $YSnCl_3$ ensembles that there is a continuum of structural parameters from $SnCl_4$ to $SnCl_3^-$. For the second problem, we classify a C atom as an X atom, i.e., as an electronegative ligand atom, when it belongs to a cyanide (or isonitrile or fulminate) group or is part of a *hapto* system. A complete list of compounds

(4) Van Kotin, G.; Noltes, J. G. In "Organotin Compounds: New Chemistry and Applications"; Zuckerman, J. J., Ed.; ACS: Washington, DC, 1976; pp 275–289.

(5) (a) Bürgi, H. B. *Angew. Chem., Int. Ed. Engl.* **1975**, *14*, 460–473. (b) Dunitz, J. D. *Philos. Trans. R. Soc. London, Ser. B* **1975**, *B272*, 99–108. (c) Dunitz, J. D. "X-Ray Analysis and the Structure of Organic Molecules"; Cornell University Press: Ithaca, NY, 1979; Chapter 7.

(6) Bürgi, H. B. *Inorg. Chem.* **1973**, *12*, 2321–2325.

(7) Gielen et al.[3] have shown that the racemization of triorganotin halides in the presence of nucleophiles, N, is a third-order process, first-order with respect to R_3SnX and second-order with respect to N. The mechanism which they suggest, and with which we agree, involves only five-coordinated species. It is not the three-body collision envisaged in the direct change from four- to six-coordination.

(8) Although the designations "inversion" and "retention" of configuration are inappropriate here, the path through intermediate a is analogous to the path with inversion in the five-coordinate case, and the path through intermediate b is analogous to the path with retention.

(9) (a) Kennard, O.; Watson, D. G.; Allen, F. H.; Motherwell, W.; Town, W. G.; Rodgers, J. *Chem. Brit.* **1975**, *11*, 213–216. (b) Allen, F. H.; Bellard, S.; Brice, M. D.; Cartwright, B. A.; Doubleday, A.; Higgs, H.; Hummelink, T.; Hummelink-Peters, B. G.; Kennard, O.; Motherwell, W. D. S.; Rodgers, J. R.; Watson, D. G *Acta Crystallogr., Sect. B* **1979**, *B35*, 2331–2339. For discussions of the use of these files see also (c) Murray-Rust, P.; Motherwell, S. *Ibid.* **1978**, *B34*, 2518–2526. (d) Murray-Rust, P.; Bland, R. *Ibid.* **1978**, *B34*, 2527–2533. (e) Murray-Rust, P.; Motherwell, S. *Ibid.* **1978**, *B34*, 2534–2546. (f) Truter, M. R. *Mol. Struct. Diffr. Methods* **1978**, *6*, 93–116. (g) Murray-Rust, P. *Ibid.* **1978**, *6*, 154–182. (h) Wilson, S. R.; Hoffman, J. C. *J. Org. Chem.* **1980**, *45*, 560–566.

(10) Zubieta, J. A.; Zuckerman, J. J. *Prog. Inorg. Chem.* **1978**, *24*, 251–475.

(11) Harrison, P. G. In "Organotin Compounds: New Chemistry and Applications", Zuckerman, J. J., Ed.; ACS: Washington, DC, 1976; pp 258–274.

(12) Murray-Rust, P.; Bürgi, H. B.; Dunitz, J. D. *J. Am. Chem. Soc.* **1975**, *97*, 921–922.

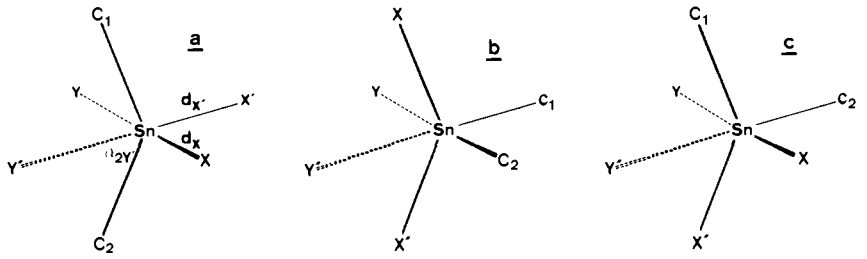

Figure 2. Possible directions of approach of two nucleophilic groups Y and Y′ to SnR_2XX' (only the C atoms bonded to Sn are shown in each R group): *a*, both Y's opposite X; *b*, both Y's opposite R; *c*, Y opposite X, Y′ opposite R. Note that the presence of X and Y in the same bidentate ligand is possible for any of these.

included in each of the following classes is provided in Supplementary Table S1 under their Cambridge Crystallographic Database acronyms.[13]

SnZ_4. Seventeen examples: two SnX_4, ten $SnMX_3$, two SnM_2X_2, three SnM_4. The scarcity of SnX_4 examples is in keeping with the idea that electronegative substituents led to an increase in coordination number. In the two SnX_4 examples that do occur, the ligands are bulky groups.

$SnCZ_3$. Three examples: two $SnCX_3$, one $SnCMX_2$.

SnC_2Z_2. Twenty-six examples: fourteen SnC_2X_2, one SnC_2MX, eleven C_2M_2. The correlation between bond angles and electronegativity of X and M is examined later.

SnC_3Z. Thirty-three examples: twelve SnC_3X and twenty-one SnC_3M. The correlation between the bond angles and the electronegativity of X or M is examined later.

SnC_4. Fourteen examples. For certain purposes we shall want to regard these as members of the SnC_2X_2 and SnC_3X classes.

SnZ_5. Three examples: two SnX_5 and one $SnSn_3O_2$. The latter will be considered with the SnC_3X_2 examples.

$SnCZ_4$. Six examples: three $SnCX_4$ and three $SnCMX_3$.

SnC_2Z_3. Seven examples: six SnC_2X_3 and one SnC_2SnO_2. The latter will be considered with the SnC_3O_2 examples. The six SnC_2X_3 examples are all approximately trigonal bipyramidal with the C atoms in two of the equatorial positions. They will be considered later in connection with possible pathways from four- to six-coordination.

SnC_3Z_2. Forty-nine examples: all SnC_3X_2 and approximately trigonal bipyramidal. Forty-three have the C atoms in the three equatorial positions. These, plus the SnC_3X examples map the pathway for the S_N2 reaction

$$SnC_3X + Y \rightleftharpoons [SnC_3XY] \rightleftharpoons SnC_3Y + X$$

with inversion of configuration. The remaining six examples have one C atom at an apical position. They will be used to explore the pathway for the S_N2 reaction with retention of configuration, but there are not really enough examples.

SnZ_6. Twenty-eight examples: twenty-seven SnX_6 and one SnM_2X_4. There are too few SnX_4 and SnX_5 examples (only two each) to map pathways between these and SnX_6. Possible pathways for expanding SnX_6 to SnX_8 are considered briefly.

$SnCZ_5$. Two examples: both $SnCX_5$.

SnC_2Z_4. Forty-five examples: all SnC_2X_4. We shall discuss the ligands as if they were near the corners of a regular octahedron although some of the distortions are actually very large. In forty-two cases the C–Sn–C angle is greater than the tetrahedral angle and we refer to these ensembles as having a transoid arrangement of the C atoms, corresponding to the approach shown in Figure 2a (in 10 cases the Sn atom actually lies on a crystallographic center of symmetry). We shall use these together with the SnC_2X_2 examples to map the path for the reaction

$$SnC_2X_2 + 2Y \rightleftharpoons [SnC_2X_2Y_2] \rightleftharpoons SnC_2Y_2 + 2X$$

The two Y ligands may be added in a concerted fashion (S_N3) or one at a time (successive S_N2 steps), and we shall consider both possibilities. We shall also look at possible reaction paths through the intermediate where the two C atoms are cis, although such examples are too few for a mapping.

(13) See paragraph at end of paper regarding supplementary material.

Table I. Sn–C Bond Lengths[a] (Å)

Sn environment	no. of examples	⟨Sn–C⟩[b]	std dev of sample
SnC_4	12	2.149	0.035
SnC_3M[c]	17	2.154	0.032
SnC_3X	13	2.140	0.030
SnC_2X_2	11	2.135	0.035
SnC_2M_2			
SnC_3O_2	20	2.139	0.041
SnC_3XY[d]	16	2.152	0.047
$SnC_2X_2Y_2$ ($\sim D_{2h}$)	10	2.127	0.048
SnC_2O_4 ($\sim C_{2v}$)	11	2.123	0.027
$SnC_2X_2Y_2$[d] ($\sim C_{2v}$)	17	2.145	0.049
SnX_4 (all)	53	2.146	
SnX_5 (all)	36	2.145	
SnX_6 (all)	38	2.134	

[a] M signifies a metal atom bonded to Sn, X an electronegative atom. [b] All bond lengths given equal weight in the averaging. [c] Two compounds, $Ph_3SnSnNO_3$ and $(Ph_3Sn)_3SnNO_3$, have been omitted from the averaging. For these ⟨Sn–C⟩ = 1.958 (25) Å; these appear to be a class apart for no obvious reason. [d] X or Y or both not oxygen.

SnZ_7. Six examples: all SnX_7. The arrangements are all approximately pentagonal bipyramidal.

SnC_2Z_5. Six examples: all SnC_2X_5. The arrangements are all approximately pentagonal bipyramidal with C atoms at the two apical positions. The reaction path $SnC_2X_4 + X \rightleftharpoons SnC_2X_5$ will be considered briefly.

SnZ_8. Six examples: all SnX_8. These have approximate dodecahedral arrangements, except for tin(IV) phthalocyanine where an Archimedean antiprismatic arrangement is forced by the shape of the ligands. The dodecahedral examples will be considered as part of the $SnX_6 + 2X \rightleftharpoons SnX_8$ reaction path.

Bond Lengths

Bond Length–Bond Order Relationships. Pauling[14] proposed a simple relationship between bond length and bond order[15]

$$\Delta d(n) = d(n) - d(1) = -c \log n \qquad (1)$$

where $d(n)$ is the bond length, $d(1)$ is the single bond length, and the value of c depends on the type of bond. The bond order so defined has no particular theoretical significance and is not to be confused with the bond order of molecular orbital theory. Nevertheless, the Pauling relationship, combined with the assumption of bond-order conservation,[19] has proved itself to be capable in

(14) Pauling, L. *J. Am. Chem. Soc.* **1947**, *69*, 542–553.

(15) An alternative relationship between bond order and bond length, $n = [d(n)/d(1)]^{-N}$, where N is an empirical constant, has been used by Brown and Shannon.[16] These authors identify the sum of bond orders about a given atom with the valence of that atom, an assumption that goes back to Pauling's 1929 electrostatic valence rule[17] and is clearly equivalent to a kind of bond-order conservation. Allman[18] has shown that the two relationships fit a large body of experimental data about equally well. We prefer eq 1 since it can be used to compare bonds involving different elements in a way that the Brown–Shannon equation does not permit.

(16) (a) Brown, I. D.; Shannon, R. D. *Acta Crystallogr., Sect.* A **1973**, *A29*, 266–282. (b) Brown, I. D. *Chem. Soc. Rev.* **1978**, *7*, 359–376.

(17) Pauling, L. *J. Am. Chem. Soc.* **1929**, *51*, 1010–1026.

(18) Allmann, R. *Monatsh. Chem.* **1975**, *106*, 779–793.

many cases of reproducing experimental reaction paths[5] and theoretical ones.[20]

Standard Bond Lengths. In principle the single-bond distance $d(1)$ for each pair of elements should be adjusted along with c (eq 1). However, one does not go far wrong in using standard distances given by the usual covalent radii[21] plus the Schomaker–Stevenson correction[22] for differences in electronegativity. These standard Sn–X single-bond distances are as follows: X = C, 2.10 Å; N, 1.98 Å; O, 1.90 Å; F, 1.83 Å; S, 2.38 Å; Cl, 2.29 Å; Se, 2.50 Å; Br, 2.45 Å; Sn, 2.80 Å; I, 2.69 Å.

Sn–C Bond Lengths. We are unable to detect any systematic variation in the Sn–C bond lengths. Table I shows the average Sn–C bond lengths in various classes of tin environments and the corresponding sample standard deviations. There do not appear to be any significant differences from one class to another.[23]

Value of c for Sn–X Bonds. For any particular Sn(IV) ensemble we can determine a value of c from eq 2, obtained by assuming

$$\sum n = \sum 10^{-\Delta d/c} = 4.00 \qquad (2)$$

that the sum of bond orders is constant, an assumption that at least has the merit of simplicity. Since we are concerned mainly with the variation in Sn–X bond lengths, we can further simplify matters by taking bond orders of Sn–C and Sn–Sn bonds to be unity. The Δd values in the remaining bonds then fix c. Average values of c determined in this way for the different SnC_nX_m classes are listed in Table S2 (individual c values are in Table S1).[13]

For those ensembles where there are two or three carbon atoms, c = 1.20 Å matches the experimental data satisfactorily, and we shall use this value hereafter. For those ensembles with one carbon atom or none, a somewhat lower value seems to be required, suggesting that (1) and (2) are too simple or that the $d(1)$ values need adjustment.[24] Another set of covalent radii might give a better fit, but the scatter is such that any improvement could only be minor.

The value of c also shows a slight dependence on the range in Δd values. That is, if the Δd values in a particular SnC_2X_4 or SnC_3X_2 ensemble are nearly equal, the c value tends to be slightly lower than when the Δd values differ greatly. In spite of these blemishes, it is astonishing how well the simple model with c = 1.20 Å works.

Correlations and Reaction Paths

There are three aspects to the correlations: first, recognizing them; second, describing them analytically; third, relating the analytical expressions to theoretical models. Since the correlations involve relatively complex systems, there is of course no reason why they should be describable by simple analytical expressions nor why they should fit simple models. Our analytical expressions and interpretations may well be short-lived, but the correlations themselves should be more durable.

Before discussing correlations among the structural parameters for the various classes of ensembles, we take up some involving that ubiquitious but damned elusive parameter, the electronegativity.

Bond Angles and Electronegativity. (a) R_3SnX Molecules. We would expect R_3SnX ensembles to have approximate C_{3v} symmetry

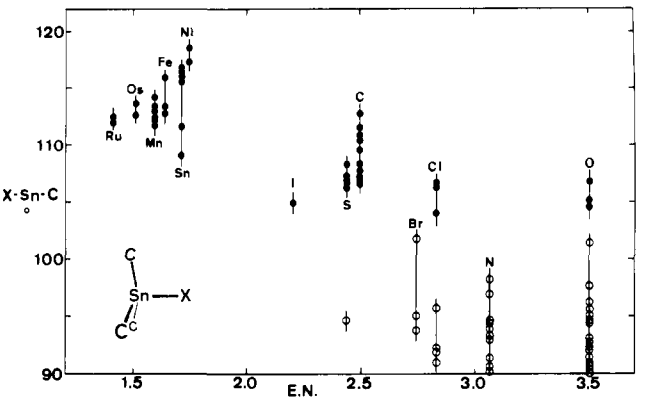

Figure 3. X–Sn–C angle vs. electronegativity of X for SnR_3X molecules (solid points). X–Sn–C angles in $YSnR_3X$ ensembles are shown by the open points.

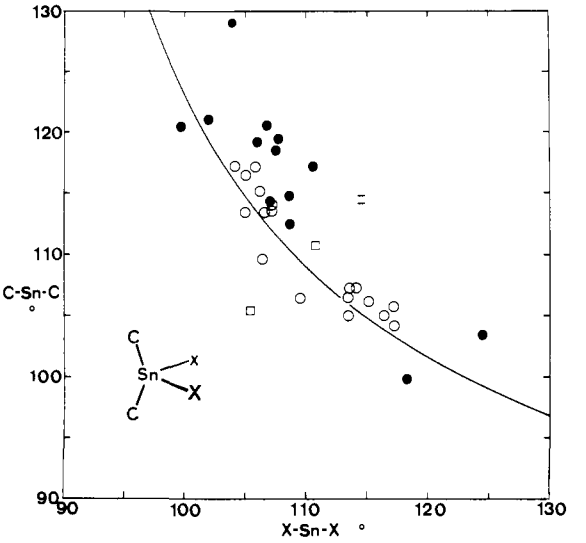

Figure 4. X–Sn–X (α_1) vs. C–Sn–C (α_2) for SnR_2X_2 molecules (solid circles), SnR_4 molecules (open circles), SnR_4 molecules with crystallographic D_{2d} symmetry (open squares). The curve shows the function $\cos\alpha_1 - 3\cos\alpha_1\cos\alpha_2 + \cos\alpha_2 = -1$.

and the C–Sn–X angle (or the average C–Sn–X angle if the symmetry is not exact) to vary with the electronegativity of X; the more electronegative X is, the smaller should be the C–Sn–X angle (the larger the C–Sn–C angle). This is the trend expected from the valence-shell electron-pair repulsion model[25] and from Bent's rule[26] and observed in $SnCl_3X$ ensembles.[12] Ho and Zuckerman[27] have commented on this effect in organotin compounds. In Figure 3 the average C–Sn–X angle is plotted against the electronegativity of X.[28] The expected trend can be discerned, but the importance of other factors is indicated by the appreciable spread of the average C–Sn–X angles for constant X.[31]

The C–Sn–X angles in SnR_3XY ensembles are also shown in Figure 3; in spite of the large spread in bond angle, the points for R_3SnX molecules do not quite extend into the range covered

(19) Johnston, H. S. *Adv. Chem. Phys.* **1960**, *3*, 131–170.
(20) (a) Agmon, N. *Chem. Phys. Lett.* **1977**, *45*, 343–345. (b) Agmon, N. *J. Chem. Soc., Faraday Trans. 2* **1978**, *74*, 388–404. (c) Eisenstein, O.; Dunitz, J. D. *Isr. J. Chem.* **1980**, *19*, 292–298.
(21) Pauling, L. "The Nature of the Chemical Bond", 3rd ed.; Cornell University Press: Ithaca, NY, 1960.
(22) Schomaker, V.; Stevenson, D. P. *J. Am. Chem. Soc.* **1941**, *63*, 37–40.
(23) If we divide the five-coordinate examples in Table I into two groups according to the R values reported in the individual crystal structure analyses, there is no significant difference in the scatter of Sn–C bond lengths. For the 19 analyses with $R \leq 6\%$ ⟨Sn–C⟩ = 2.135 (38) Å and for the 17 analyses with $R \geq 6\%$ ⟨Sn–C⟩ = 2.156 (40) Å. The scatter is essentially the same suggesting that it originates from an intrinsic spread rather than from the variable quality of the analyses.
(24) It should be recognized that the value of c is sensitive to the d(1) values used, and that this sensitivity decreases with the number of bonds. Decreasing d(1) by 0.04 Å would increase the ⟨c⟩ values in Table S2 by 57, 28, 19, and 12% for SnX_5, SnX_6, SnX_7, and SnX_8, respectively.
(25) Gillespie, R. J. "Molecular Geometry"; Van Nostrand-Reinhold: London, 1972.
(26) Bent, H. A. *Chem. Rev.* **1961**, *61*, 275–311.
(27) Ho, Y. K.; Zuckerman, J. J. *J. Organomet. Chem.* **1973**, *49*, 1–84.
(28) Electronegativity values from Allred and Rochow[29] as augmented by Cotton and Wilkinson.[30]
(29) Allred, A. L.; Rochow, E. G. *J. Inorg. Nucl. Chem.* **1958**, *5*, 264–268.
(30) Cotton, F. A.; Wilkinson, G. "Inorganic Chemistry", 3rd ed.; Interscience: New York, 1972, p 115.
(31) Another expression of spread is the difference, δ, between the largest and smallest C–Sn–X angle in each molecule. The average value of δ for the R_3SnX molecules used in Figure 3 (excluding R_4Sn) amounts to 5.4°. In all but one example the three R groups are the same, so that, except for packing effects, we would expect δ to be 0.

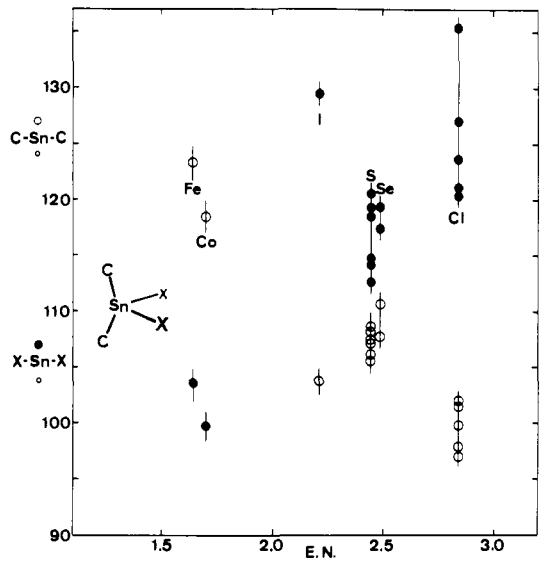

Figure 5. X-Sn-X (α_1) and C-Sn-C (α_2) vs. electronegativity of X and SnR_2X_2 molecules.

by corresponding R_3SnXY ensembles.

(b) SnR_2X_2 Molecules. Along similar lines we would expect the bond angles in R_2SnX_2 to depend on the electronegativity of X. Here the situation is more complicated in that for C_{2v} symmetry there are three kinds of angles, two of which are independent. According to the simple hybridization model,[32] the angles α_1 = X-Sn-X and α_2 = C-Sn-C should be related by $\cos\alpha_1 - 3\cos\alpha_1\cos\alpha_2 + \cos\alpha_2 = -1$ (which is hardly distinguishable within the observed range from the still simpler relationship $\cos\alpha_1 + \cos\alpha_2 = -{}^2/_3$). The experimental results for R_2SnX_2 molecules are shown in Figure 4.

The R_4Sn molecules (open circles) follow the angle relationship well, except where the molecule has crystallographic D_{2d} symmetry (open squares). The R_2SnX_2 molecules do not follow the relationship as well; the sum of the two angles tends to be too large. Figure 5 shows the dependency of the angles on the electronegativity of X. As in the R_3SnX molecules, the C-Sn-C angle tends to increase as the electronegativity of X increases. The spread in angle is again large. The angles obviously depend on other factors besides electronegativity, which, in any case, can hardly be regarded as a particularly well-defined parameter. It is discouraging, for example, that any smooth curves drawn through the X-Sn-X and C-Sn-C points would not cross at the electronegativity of carbon.

Structural Correlations for SnC_3XY Ensembles with Trans X, Y. The S_N2 Pathway for Substitution with Inversion at Tetrahedral Sn. Most of our examples of five-coordinate Sn(IV) have local composition SnC_3XY with local symmetry approximately C_{3v}. Two correlations are found: as the Sn-Y distance d_Y becomes shorter, the Sn-X distance d_X tends to become longer and the X-Sn-C angles tend to become smaller. Figure 6 shows the interdependence of Δd_Y and Δd_X. Points marked by filled circles indicate that both X and Y are oxygen atoms; open circles indicate that at least one is not oxygen. The two distributions are similar, showing that the standard bond distances are mutually consistent. The solid curve shows the bond-order conservation function

$$10^{-\Delta d_X/c} + 10^{-\Delta d_Y/c} = 1 \qquad (3)$$

with c = 1.20 Å.

The second correlation, between distance and angle, can be expressed in terms of the average C-Sn-X angle (α_X).[33] Figure

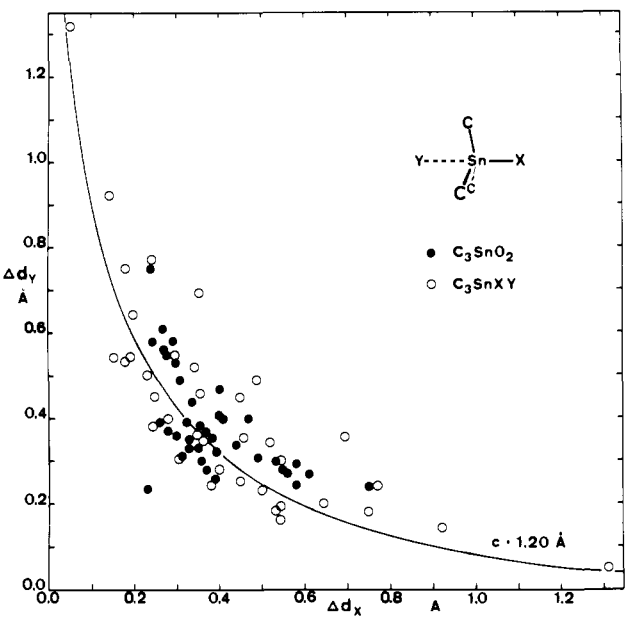

Figure 6. Δd_Y vs. Δd_X for SnC_3XY ensembles. The curve gives eq 3 with c = 1.20 Å.

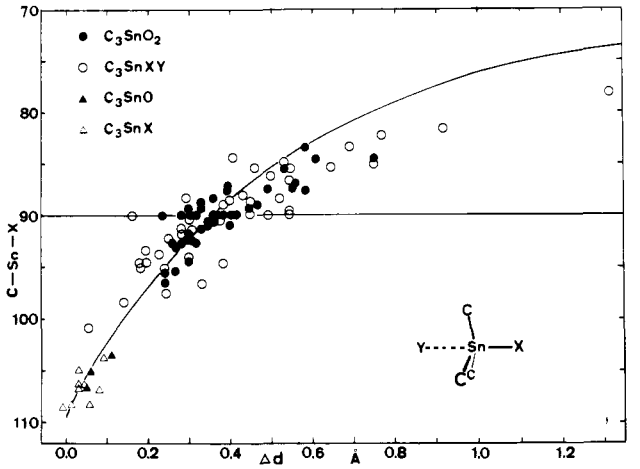

Figure 7. C-Sn-X (α_X) and C-Sn-Y (α_Y) vs. Δd_X and Δd_Y for SnC_3XY ensembles. The curve gives the combination of eq 1, 3, and 4 with c = 1.20 Å.

7 shows the dependence of Δd_X and Δd_Y on α_X. For the dependence of bond order on bond angle, we follow Bürgi[5a,6] and assume

$$n_X = (1 - 3\cos\alpha_X)/2 \qquad (4a)$$

$$n_Y = (1 + 3\cos\alpha_X)/2 \qquad (4b)$$

so that $n_X = 1$ when α_X is the tetrahedral angle and $n_X = {}^1/_2$ when $\alpha_X = 90°$. The solid curve in Figure 7 shows the relationship between Δd_X, Δd_Y, and α_X with c = 1.20 Å as before.

The coupling between bond length changes and bond angle changes during the passage from tetrahedral to trigonal-bipyramidal coordination (S_N2 pathway) is very similar to that found by Bürgi[6] for the CdS_3XY system. Like the latter, it can be described analytically by a simple expression derived from the Pauling relationship (eq 1) and the assumed relationship between bond orders and α_X given in eq 4.

Structural Correlations for SnC_3XY Ensembles with Cis X_3 Y. The S_N2 Pathway for Substitution with Retention at Tetrahedral Sn. When the X and Y atoms in an SnC_3XY ensemble are part of a bidentate ligand two different arrangements are possible. The bidentate ligand can act as a bridging group, in which case the C_{3v} arrangement of the SnC_3XY ensemble with trans X, Y occurs without exception. Analogously, S_N2 reactions take place with inversion only if the entering and leaving atoms are on two different molecules. Alternatively, the bidentate ligand can act as a chelate,

(32) Mislow, K. "Introduction to Stereochemistry"; W. A. Benjamin: New York, 1965, p 16.

(33) The average C-Sn-C angle (α_C) or the displacement (Δd_Z) of the Sn atom from the plane defined by the three C atoms could be used as well. For exact C_{3v} symmetry these are related by $\cos\alpha_X = -[(2\cos\alpha_C + 1)/3]^{1/2} = \Delta d_Z/d_C$.

Table II. SnC_3X_2 Examples with *cis*-X_2

compd	Sn environment	chelate ring	Δd_X, Å	Δd_Y, Å	C_1-Sn-X, deg	X-Sn-Y, deg	Y-Sn-C_1, deg
TCHSNA	SnC_3O_2	SnOCO	0.22	1.05	95	45	140
MCARSN	SnC_3S_2	SnSCS	0.09	0.94	94	60	154
MCARSN	SnC_3S_2	SnSCS	0.09	0.78	95	63	153
TPSNBH10	SnC_3O_2	SnOCNO	0.19	0.41	87	71	157
PPTPSN	SnC_3O_2	SnOCCCO	0.19	0.38	86	78	164
NTPSNT10	$SnSn_3O_2$	SnONO	0.69	0.70	86	42	128

in which case X and Y must occupy cis positions of the trigonal bipyramid, giving an arrangement whose highest possible symmetry is C_s. Just as X and Y must be in the same chelate group for S_N2 substitution[34] to occur with retention of configuration, this also appears to be a requirement for the cis X, Y arrangement to be found in the solid state.

Only seven examples of the cis X, Y arrangement are known to us (including one where there is a discrepancy between the published angles and those calculated from the coordinates). Some data for the six remaining examples are given in Table II. Regularities are obscured by the variable bite angle in the chelate groups, and there are too few data to map out the path in detail. However, the local threefold axis of the SnR_3 fragment tends to lie close to the SnXY plane with one carbon atom C(1) almost in this plane; as Δd_Y becomes smaller, the C(1)–Sn–X angle tends to become smaller, as might be expected.

The $SnSn_3O_2$ example contains some interesting features. The two Sn–O distances are longer than we would expect from eq 1 with c = 1.20 Å; to make up for this the Sn–Sn distances are shorter than normal. This ensemble appears to have Sn–Sn bond orders near 1.2 and Sn–O bond orders near 0.2. It is also the only one with two equal Sn–X distances, and hence it must lie close to the symmetric intermediate or transition-state structure. Although the Sn–O distances are equal, the two O atoms are not equivalent. The plane of the two O atoms and the central Sn atoms contains one of the Sn substituents; to make the two O atoms equivalent, the $SnSn_3$ group would have to be rotated 30° around its local threefold axis. The extrapolation, that the structure with symmetry-equivalent O atoms corresponds to the transition state (i.e., energy maximum) and not to an intermediate (i.e., local energy minimum) along the S_N2 retention pathway, seems hardly warranted by the data—but is irresistible. Indeed, one might go even further. The symmetric situation, with the threefold axis of the SnR_3 grouping coincident with the twofold axis of the SnX_2 grouping, represents the same kind of deformation of a trigonal bipyramid as has been postulated to occur at the midpoint of the turnstile rotation mechanism.[35] None of our examples show this structure, all having approximately planar $CSnX_2$ arrangements. It appears, at least for Sn(IV), that the turnstile does not turn readily.

Recent NMR and X-ray studies[36] of two silyl nitronate esters reveal structures that lean toward an S_N2 retention pathway at silicon, having many features in common with the R_3SnXY examples described above. The silyl esters in question show rapid silyl migration from one oxygen to the other.

Trends in SnC_2XYZ Ensembles. There are seven examples of this local composition, where X, Y, and Z are variously N, O, S, and Cl. They are all approximately trigonal bipyramidal with the C atoms in equatorial positions; we take the Z atom to be at the other equatorial position. This set of examples does not show any clearcut trends. The C–Sn–Z angles are significantly less that 120° in four examples but larger in three. In two examples

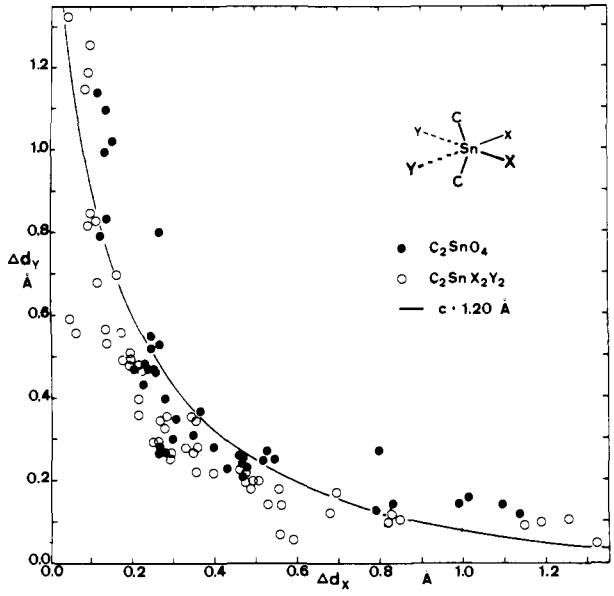

Figure 8. Δd_Y vs. Δd_X for $SnC_2X_2Y_2$ ensembles. The curve gives eq 3 with c = 1.20 Å.

Δd_Z is greater than Δd_X, and Δd_Y, in five examples it is smaller. The SnC_2XYZ ensembles are included later in the discussion of disubstitution in SnC_2X_2 molecules.

Structural Correlations for $SnC_2X_2Y_2$ Ensembles with Transoid C, C. The S_N3 and $(S_N2)^2$ Pathways for Disubstitution at Tetrahedral Sn. For most of our examples of six-coordinated tin, the local composition is $SnC_2X_2Y_2$ with transoid C atoms and approximately C_{2v} local symmetry (see Figure 2a). These examples show certain trends in common with those found for five-coordination. There are obvious correlations between d_X and d_Y and between these distances and the C–Sn–C angle, α_{12}. In addition, we find a correlation between the X–Sn–X′ angle, $\alpha_{XX'}$, and the Y–Sn–Y′ angle, $\alpha_{YY'}$, but, surprisingly, not between $\alpha_{XX'}$ and α_{12}.

The relationship between Δd_X and Δd_Y (figure 8) is similar to that for five-coordinate Sn, and the solid curve is drawn for the same value of c = 1.20 Å as in Figure 6. In the central region a smaller value of c would give a better fit, and at the ends a larger value of c would be better, suggesting that the simple analytical expression (eq 3) could be improved on. It should be noted that the data points in Figure 8 refer to opposite pairs of bonds (for many examples, the two data points for each $SnC_2X_2Y_2$ ensemble coincide).

The angles at Sn usually show approximate C_{2v} symmetry. Of the various possible angles that could be plotted against the distances, the obvious first choice seemed to be the C–Sn–C angle, α_{12}. The correlation against distance (Figure 9) is complicated in that there are now two Δd_X distances and two Δd_Y ones, and for several examples the distances do not show approximate C_{2v} symmetry, i.e., $\Delta d_X \neq \Delta d_{X'}$, $\Delta d_Y \neq \Delta d_{Y'}$. Both distances are then shown. The smooth curve is based on c = 1.20 Å and the assumption that

$$n_X = [1 + 3^{1/2} \cos(\alpha_{12}/2)]/2 \quad (5a)$$

$$n_Y = [1 - 3^{1/2} \cos(\alpha_{12}/2)]/2 \quad (5b)$$

which makes n_X = 1 when α_{12} is the tetrahedral angle and n_X =

(34) The kinetic nomenclature is confused in this context. For retention of configuration Y must enter as X leaves; in this sense the reaction can be classified as S_N2. On the other hand X and Y belong to the same molecule so that first-order kinetics should be followed; in this sense the reaction is S_N1.

(35) Ugi, I.; Marquarding, D.; Klusacek, H.; Gillespie, P.; Ramirez, F. *Acc. Chem. Res.* **1971**, *4*, 288–296. Gillespie, P.; Hoffmann, P.; Klusacek, H.; Marquarding, D.; Pfuhl, S.; Ramirez, F.; Tsolis, E. A.; Ugi, I. *Angew. Chem.* **1971**, *83*, 691–721.

(36) Colvin, E. W.; Beck, A. K.; Bastani, B.; Seebach, D.; Kai, Y.; Dunitz, J. D. *Helv. Chim. Acta* **1980**, *63*, 697–710.

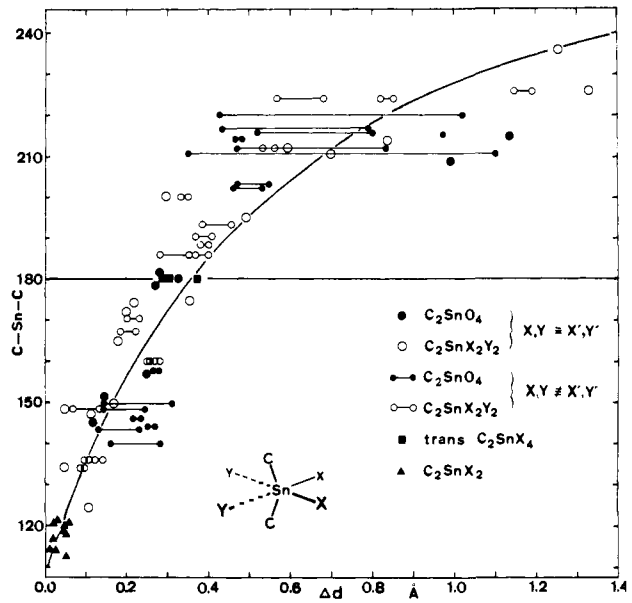

Figure 9. C–Sn–C (α_{12}) vs. Δd_X and Δd_Y for $SnC_2X_2Y_2$ ensembles. The curve gives the combination of eq 1, 3, and 5 with c = 1.20 Å.

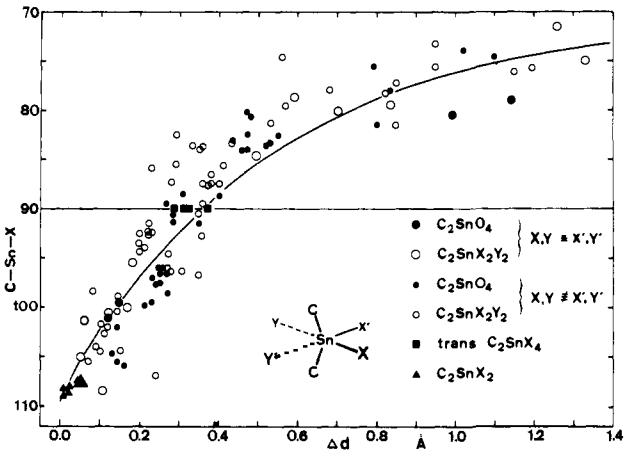

Figure 10. C–Sn–X (α_X) and C–Sn–Y (α_Y) vs. Δd_X and Δd_Y for $SnC_2X_2Y_2$ ensembles. The curve is the same as in Figure 7.

$^1/_2$ when α_{12} = 180°. Points for R_2SnX_2 molecules and for all-trans R_2SnX_4 ensembles fit the curve as well as the others do.[37]

The examples with Δd_X very different from $\Delta d_{X'}$ show that the assumption of approximate C_{2v} symmetry in Figure 9 is somewhat forced. To take account of these differences, we should correlate the average C–Sn–X angle α_X with Δd_X and Δd_Y, and the average C–Sn–X′ angle $\alpha_{X'}$ with $\Delta d_{X'}$ and $\Delta d_{Y'}$.[38] The results are shown in Figure 10. The smooth curve corresponds to the original bond order–bond angle relationship of eq 4 with c = 1.20 Å (as in Figures 8 and 9). The fit is excellent, including the points for R_2SnX_2 molecules and for all-trans R_2SnX_4 ensembles; points for three SnC_2XYZW examples have also been included. A similar improvement in fit could of course have been obtained by averaging connected pairs of points in Figure 9.[39]

However, the change in viewpoint from Figure 9 to Figure 10 is more than merely cosmetic. The majority of the examples have approximate C_{2v} symmetry ($\Delta d_X \approx \Delta d_{X'}$ and $\Delta d_Y \approx \Delta d_{Y'}$). These examples map a path for the symmetric addition of two ligands Y to a tetrahedral SnR_2X_2 molecule to give an octahedral ensemble that would be an intermediate or transition state for a disubstitution reaction, which we shall refer to as an S_N3 reaction (see Figure 11). This is not a type of path we would expect to be important in solution or in the gas phase because it involves a three-body collision. However, if our structure correlation studies mean anything, the S_N3 path should surely correspond to a fairly well-defined valley in the potential energy hypersurface. Although paths of this nature, which follow potential energy valleys but are disfavoured entropically, have largely been ignored so far in discussion of chemical reactivity, they may be important for enzymatic reactions.

In addition to the symmetric double addition and elimination process (S_N3) there are at least two others that have to be considered in any discussion of the double substitution reaction. One is the consecutive addition of Y and Y′ followed by the consecutive elimination of X and X′. Figure 12 shows the first half of this process, which we call $(S_N2)^2$, although it would follow third-order kinetics. The other is: addition of Y, elimination of X, addition of Y′, elimination of X′, where only five-coordinated species are involved. This is two consecutive S_N2 reactions.

Figure 13 is an attempt to decide to what extent the unsymmetrical $SnC_2X_2Y_2$ examples with $\Delta d_Y < \Delta d_{Y'}$ (and usually $\Delta d_X > \Delta d_{X'}$) represent mere scatter from the S_N3 path and to what extent they provide information about the alternative $(S_N2)^2$ pathway: the symmetric S_N3 path lies along the diagonal with equal C–Sn–X and C–Sn–X′ angles and the majority of points (including those for tetrahedral SnC_2X_2) are close to this line. The question is: do the points that deviate much from this line do so in a systematic way, and, if so, is this way compatible with an $(S_N2)^2$ type path? Such a path involves a range of five-coordinate intermediates with $\alpha_{X'}$ going from tetrahedral to an uncertain value around 120° as α_X goes from tetrahedral to 90° (Figure 12, a to b) followed by a range of six-coordinate intermediates with α_X remaining constant at 90° while $\alpha_{X'}$ goes from its uncertain value around 120° to 90° (Figure 12, c to d).

In contrast to the large number of SnC_3XY examples for the S_N2 pathway (Figures 6 and 7), there are only six SnC_2XYZ examples which are plainly inadequate either to confirm or to contradict the proposed $(S_N2)^2$ path shown in Figure 13.

In the distribution of six-coordinate points, the three most extreme outliers from the S_N3 line straddle the second part of the $(S_N2)^2$ path at $\alpha_{X'} \approx 106°$, but this is scarcely enough to define anything. On the whole, the deviations from the S_N3 line seem to have a rather unsystematic nature, and it is difficult to draw any conclusions from them. At any rate, the experimental data define the S_N3 path better than any of the alternatives.

The remaining correlation between $\alpha_{XX'}$ and $\alpha_{YY'}$ is not shown. It is not so interesting since it gives us no information about those parts of the potential energy hypersurface relevant to reaction paths. While $\alpha_{XX'}$ varies only over a small range (70–100°), $\alpha_{YY'}$ varies over a much larger one (70–180°) and small $\alpha_{XX'}$ goes with large $\alpha_{YY'}$. Beyond this little can be said.[40] Two points with $\alpha_{YY'} < 50°$ do not fit this pattern. They come from molecules where Y and Y′ are in the same chelate group, nitrate or acetate, forming four-membered rings. Both structures could about as well be regarded as five-coordinated.

Trends in $SnC_2X_2Y_2$ Ensembles with Cis C, C. When the X and Y atoms in $SnC_2X_2Y_2$ belong to bidendate ligands, the arrangement shown in Figure 2b occasionally occurs. In contrast to five-coordination, where the cis XY arrangement is forced by chelation, a six-coordinate structure with two chelates XY and X′Y′ could have either cis or trans C atoms, (Figure 2b or 2a). Many of the examples in the preceding section correspond to such trans isomers. Only three examples with cis C atoms occur in our collection of structures. In all three cases the Δd_X values are

(37) Points for *all-trans*-$R_2SnX_2Y_2$ would also fit about as well but they are not shown since they cannot be fitted into the reaction coordinate picture.

(38) These averages (in degrees) were taken as $\alpha_X = (\alpha_{1X} + \alpha_{2X} + 360 - \alpha_{1Y} - \alpha_{2Y})/4$ to allow for nonlinearity in the X–Sn–Y arrangement.

(39) The two kinds of correlation are related but not equivalent. In an ensemble with C_{2v} symmetry the angles are related by $\cos \alpha_{XC} = -\cos(\alpha_{XX'}/2) \cos(\alpha_{12}/2)$, $\cos \alpha_{YC} = \cos(\alpha_{YY'}/2) \cos(\alpha_{12}/2)$. Thus eq 4 and 5 are equivalent only if $\alpha_{XX'}$ is the tetrahedral angle and $\alpha_{YY'}$ is its complement. This condition is clearly not met. In principle one of the two correlations could give a better fit than the other, but, given the scatter of the data, no choice can be made.

(40) Kepert, D. L. *J. Organomet. Chem.* **1976**, *107*, 49–54. Kepert has discussed this type of correlation, for a limited set of data from ensembles with chelate rings, in terms of ligand–ligand repulsions.

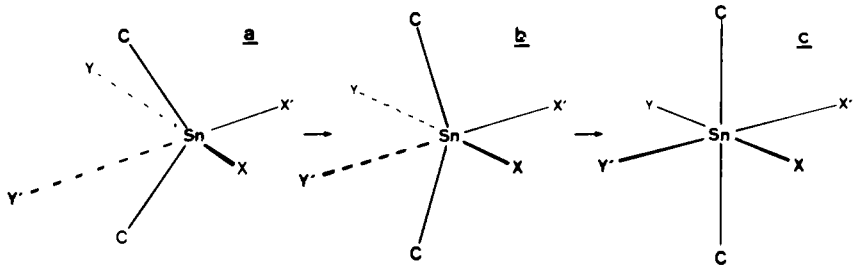

Figure 11. The S_N3 pathway: symmetric approach of 2Y to an SnR_2X_2 molecule. Only the C atoms bonded to Sn are shown in each R group.

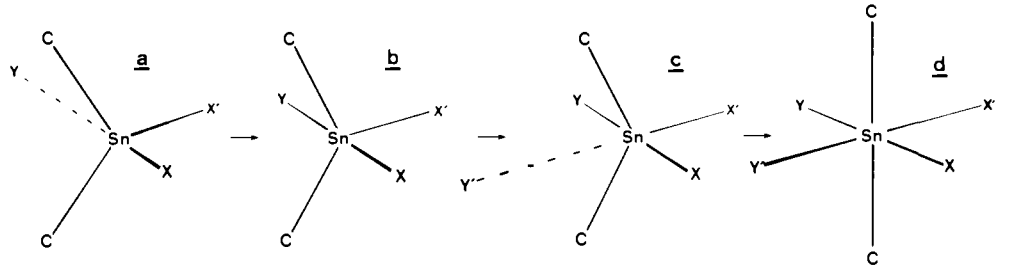

Figure 12. The $(S_N2)^2$ pathway: sequential approach of 2Y to SnR_2X_2. Only the C atoms bonded to Sn are shown in each R group.

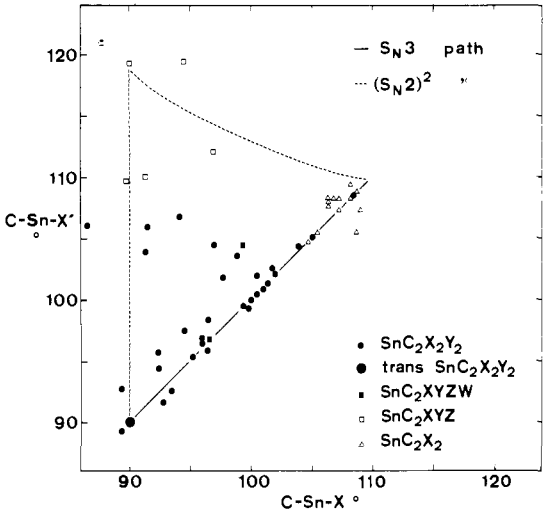

Figure 13. C–Sn–X′ ($\alpha_{X'}$) vs. C–Sn–X (α_X). The S_N3 pathway lies along the solid line. The $(S_N2)^2$ pathway lies approximately along the dotted lines.

near 0.2 Å and the Δd_Y values are near 0.4 Å. Also the C–Sn–C angle is nearer to tetrahedral than to 90°.

Trends in SnC_2X_5 Ensembles. The six examples in this class (Table S3)[13] are all approximately pentagonal bipyramidal with C atoms in the apical positions and at least one chelate ring in the X_5 set. The smallest C–Sn–C angle is 148°.

Trends in SnX_8 Ensembles. There are six examples of SnX_8 ensembles, all involving chelating ligands. In one example, SNPTCY, eight N atoms are in two phthalocyanine rings and have Archimedean antiprismatic coordination about the Sn atom. Four of the remaining five are crystallographically independent examples of the same molecule, ACETSN $[Sn(O_2CMe)_4]$, with the same dodecahedral arrangement of the eight O atoms about the Sn atom. In the last example, MDTCSN $[Sn(S_2CNMe_2)_4]$, there are six S atoms at vertices of a distorted octahedron and two more distant ones in directions leading to the dodecahedral arrangement (see Figure 14 for a highly idealized picture). In the analogous complexes DETCSN $[Sn(S_2COEt)_4]$ and EXANSN $[Sn(S_2CNEt_2)_4]$, the two distant ligands are so far from the Sn atoms that these were classed as six-coordinated with two monodentate and two bidentate ligands; the monodentate ligands are cis in both cases. These few data are consistent with the following sequence for binding four bidentate ligands to Sn. First

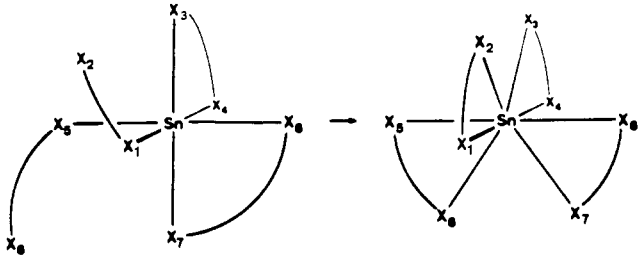

Figure 14. Possible path for increase for six- to eight-coordination with four X_2 bidentate ligands.

the six-coordinate arrangement with cis-monodentate ligands (Figure 14) forms; the two remaining ligand atoms then approach in the plane defined by its monodentate partner, the Sn atom, and another bidentate group.

An Overall Trend. When one or two additional ligands approach a tetrahedral SnX_4 molecule, the direction of approach of each ligand is always toward the center of a face, i.e., opposite to an Sn–X bond, corresponding respectively to the familiar S_N2 pathway and the less familiar S_N3 one. When one or two additional ligands approach a trigonal-bipyramidal SnC_2X_3 ensemble, the approach is toward the center of an equatorial edge, still opposite to an Sn–X bond. However, when one or two additional ligands approach an octahedral SnX_6 ensemble, where approach to the Sn atom opposite an Sn–X bond is blocked, the direction of approach of each ligand is toward the center of an edge and not toward the center of a face (see, for example, Figure 14). This pattern requires further verification, but it is consistent with all the data we have so far.

Appendix

Analogies with Ge(IV) and Pb(IV). We expect germanium to show less tendency to expand its coordination number from four and lead to show more. An examination of the Database shows fewer examples for both than with tin.

Germanium. Eighty entries in the Database cover germanium-containing compounds. Of these fifty-five describe Ge(IV) compounds and provide eighty examples of Ge(IV) atoms in various crystal environments. As with Sn, we shall briefly consider each class GeC_nZ_m. (See Supplementary Table S1 for the lists.)[13]

GeZ_4. Seventeen examples: five GeX_4, seven $GeMX_3$, five GeM_2X_2. GeX_4 examples are more abundant than SnX_4 examples (five out of fifty-five compared with two out of two hundred and forty-one!).

$GeCZ_3$. Five examples: three $GeCX_3$, two $GeCMX_2$.

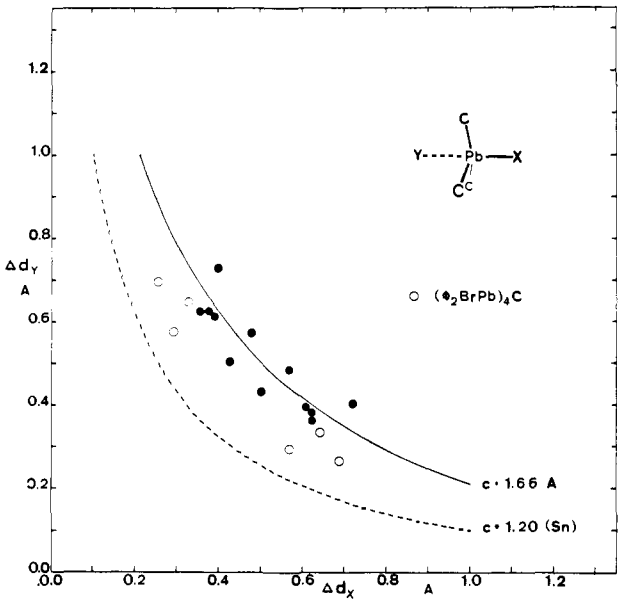

Figure 15. Δd_Y vs. Δd_X for PbC_3XY ensembles. The solid curve gives eq 3 with c = 1.66 Å. The dotted curve is for SnC_3XY ensembles. See text for discussion of the $(Ph_2BrPb)_4C$ points.

GeC_2Z_2. Sixteen examples: five GeC_2X_2, one GeC_2MX, ten GeC_2M_2. The dependence of the C–Ge–C and Z–Ge–Z angles on electronegativity is about the same as that shown for tin in Figures 3 and 4.

GeC_3Z. Thirteen examples: seven GeC_3X, six GeC_3M. Again the dependence of the average Z–Ge–C angles on electronegativity is about the same as that shown in Figure 2.

GeC_4. Fourteen examples.

GeZ_5. Six examples: five GeX_5, one $GeMX_4$.

$GeCZ_4$. Two examples: both $GeCX_4$.

GeC_3Z_2. One example. This is TMGECY [Me_3GeCN] with four approximately normal Ge–C distances and an additional N···Ge distance of 3.57 Å.

GeZ_6. Five examples: all GeX_6.

GeC_2Z_4. One example, DMCYGE [$Me_2Ge(CN)_2$], with four approximately normal distances Ge–C and two additional N···Ge distances of 3.28 and 3.83 Å.

A value of c = 0.8 Å is obtained from bond distances in the GeX_5 and GeX_6 ensembles by using eq 2. There are too few examples to attempt to describe any reaction paths. Ge(IV) shows very little tendency to increase its coordination number above four unless all of the substituents are more electronegative than carbon.

Lead. Reduction of Pb(IV) occurs more readily than that of Sn(IV) and consequently Pb(IV) compounds are less common than Sn(IV) ones. Nevertheless, we would expect their structural chemistry to be similar.

Most of the sixty-three structures of lead compounds listed in the Database involve Pb(II) or lower oxidation states. There are only thirteen Pb(IV) compounds, including seventeen different Pb atoms, for which coordinates are available: four PbC_3Z, one PbC_4, one PbC_2Z_3, nine PbC_3Z_2, one PbC_2Z_4, one PbC_2Z_6 (see Supplementary Table S1).[13]

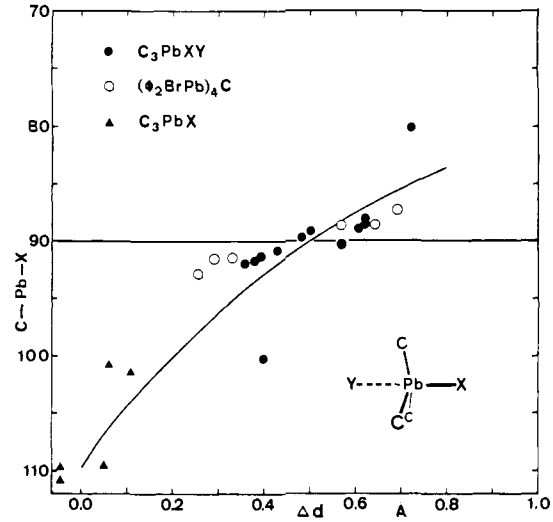

Figure 16. C–Sn–X (α_X) and C–Sn–Y (α_Y) vs. Δd_X and Δd_Y for PbC_3XY ensembles. The curve gives the combination of eq 1, 3, and 4 with c = 1.66 Å.

The average Pb–C bond distances are the same within experimental error for four-coordination (five examples), 2.205 (58) Å and five-coordination (nine examples), 2.192 (46) Å. A plot of Δd_X vs. Δd_Y for the five-coordinate compounds is shown in Figure 15 and a plot of Δd_X and Δd_Y vs. α_X is shown in Figure 16. The reference Pb–X distances used are as follows: X = C, 2.14 Å; N, 2.01 Å; O, 1.94 Å; Cl, 2.33 Å; Br, 2.49 Å. From six of the nine examples we find c = 1.66 (10) Å, significantly larger than for Sn(IV). The three remaining examples concern PBRPBM [tetrakis(diphenylbromoplumbyl)methane], where the d_Y distances are intramolecular. In general Δd_X and Δd_Y are more nearly equal than with Sn(IV) but this may merely reflect the limited amount of data. There is only one example of six-coordinate Pb(IV), DPDCPB (diphenyldichlorolead). The lead atom lies on a crystallographic center of symmetry; Δd_X = 0.47 Å for the four Pb–Cl distances, about the same as was found in five-coordination.

Acknowledgment. This work was carried out with the financial support of the Swiss National Science Foundation.

Supplementary Material Available: Listings of the compounds used, identified by their Cambridge Crystallographic Database code (Table S1), average values of c for the various SnC_nX_m classes (Table S2), and bond angle information for six SnC_2X_5 compounds (Table S3) (16 pages). Ordering information is given on any current masthead page.